Lasers in Manufacturing Conference 2017

Experimental investigation of a process chain combining sheet metal bending and laser beam melting of Ti-6Al-4V

Lorenz Butzhammer[a,c], Patrick Dubjella[b], Florian Huber[a,c,*], Adam Schaub[b], Markus Aumüller[a], Alexander Baum[a], Oleksandra Petrunenko[b], Marion Merklein[b], Michael Schmidt[a,c]

[a] *Institute of Photonic Technologies (LPT), Friedrich-Alexander-Universität Erlangen-Nürnberg, Konrad-Zuse-Straße 3-5, 91052 Erlangen, Germany*

[b] *Institute of Manufacturing Technology, Friedrich-Alexander-Universität Erlangen-Nürnberg, Egerlandstraße 13, 91058 Erlangen, Germany*

[c] *Erlangen Graduate School in Advanced Optical Technologies (SAOT), Paul Gordan Straße 6, 91052 Erlangen, Germany*

Abstract

In spite of several advantages such as a great freedom of design, comparatively long process times are a major drawback in additive manufacturing technologies such as laser beam melting (LBM) of metal powder. A strategy to overcome this limitation is to combine additive manufacturing with other promising manufacturing concepts. In this paper, we characterize hybrid components manufactured using a consecutive process chain including warm bending of Ti-6Al-4V sheets and LBM. With the additive process a functional structure is built on top of the bending zone using powder from the same material. As a measure for the connection strength, shear tests were performed. The shear strength is analyzed for both possible process routes of forming and LBM. Therefore a modular clamping device for bent sheets was developed in order to enable simultaneous production of additive parts on several bent sheets with different thicknesses and radii. Results show that the formability of sheets is strongly influenced by the sequence of the process route, while no significant difference in shear strength of the connection was observed, even if the energy density in the LBM process is varied to a large extent. The post heat treatment is discussed as major cause, as homogenization of the microstructure takes place, although the applied temperature is beneath the beta transus temperature.

Keywords: Laser Beam Melting; Additive Manufacturing; Bending; Titanium Alloys

* Corresponding author. Tel.: +49-9131-85-64103; fax: +49-9131-85-23234.
E-mail address: florian.huber@lpt.uni-erlangen.de.

1. Introduction

Laser beam melting (LBM) of metals in powder bed is an innovative manufacturing technology. A workpiece is additively built by selectively melting micro-sized metal powder layer by layer using a focused laser beam. This leads to advantages like a high flexibility and a great freedom of design, which gives the possibility to produce structures that are not producible using conventional manufacturing technologies. In the case of expensive or hard-to-machine materials such as Ti-6Al-4V, LBM can become competitive to machining even for simpler structures. Here, the advantage can be used that the part design can easily be modified and therefore weight can be reduced by topology optimization. This is of major interest in aerospace industry.

However, long process times and the resulting high costs for larger production series often prevent the application of the technology. Machine cost, based on the machine hour rate, has the biggest share on overall costs (Schrage, 2016). Thus, efforts are undertaken to reduce the process time. To a certain extent, this can be achieved by using multiple laser sources. Another strategy is to combine LBM with other manufacturing technologies. Sheet metal forming is a promising production technique for combination with LBM in a successive process chain. Besides short process times, it offers the advantage of low costs for mass production and the ability to process large scaled parts. (Schaub et al., 2016) showed that for simple test geometries on flat ground the build time for LBM can be reduced by 55 to 75 % by building directly on sheet metal. To be able to produce more complex structures, sheet metal forming can be performed before or after the LBM process, resulting in a hybrid structure.

In this paper, Ti-6Al-4V is used as powder as well as sheet material. Because of its good weight to strength ratio, Ti-6Al-4V has become a popular material in the aerospace industry. Another field of application is the medical implant sector, as this alloy shows a good biocompatibility and corrosion resistance. In this sector LBM as well as electron beam melting is well-established as it also gives the possibility to produce systematic porous structures for improved osseointegration (Matena et al., 2015). Hip and knee implants are some examples which are already put into practice.

In former work, deep drawing was used as forming technique as part of the hybrid process (Ahuja et al., 2015). Laser beam melted cylindrical pins were placed in the center on the top side of a deep drawn cup. In order to investigate the interaction of forming and laser beam process and the influence of residual stresses in the building area in more detail, (Merklein et al., 2016) introduced bending as possible forming process in the hybrid process chain. As the laser beam melted structure is positioned directly on the stress loaded extreme fiber, the influence of the forming process is assumed to be more prominent.

In this paper both possible process routes of warm bending and LBM are investigated. Bending is performed either before or after LBM. To be able to use bent sheets as substrate in the LBM process, a new concept for clamping had to be developed. It is demonstrated that this modular concept enables simultaneous production of additive parts on several bent sheets with different thicknesses and radii. The differences of the two possible process chains are shown in terms of metallographic analysis and mechanical shear tests as a measure of the connection strength.

2. Methods

2.1. Process chain

There are two different consecutive process routes to produce a hybrid part combining sheet metal bending and LBM. This is shown in Fig. 1 a). Both routes lead to a hybrid sample consisting of a sheet substrate and an additively built pin at top of the bending zone. Both possible sequences are investigated in

this paper using Ti-6Al-4V as material for the sheet as well as for the powder in the LBM process. Metal sheets from the same batch act as starting point for both routes. Sheet thicknesses of 1 mm and 1.5 mm were used for preliminary tests. For metallographic analysis and mechanical testing samples with a sheet thickness of 1.5 mm are shown.

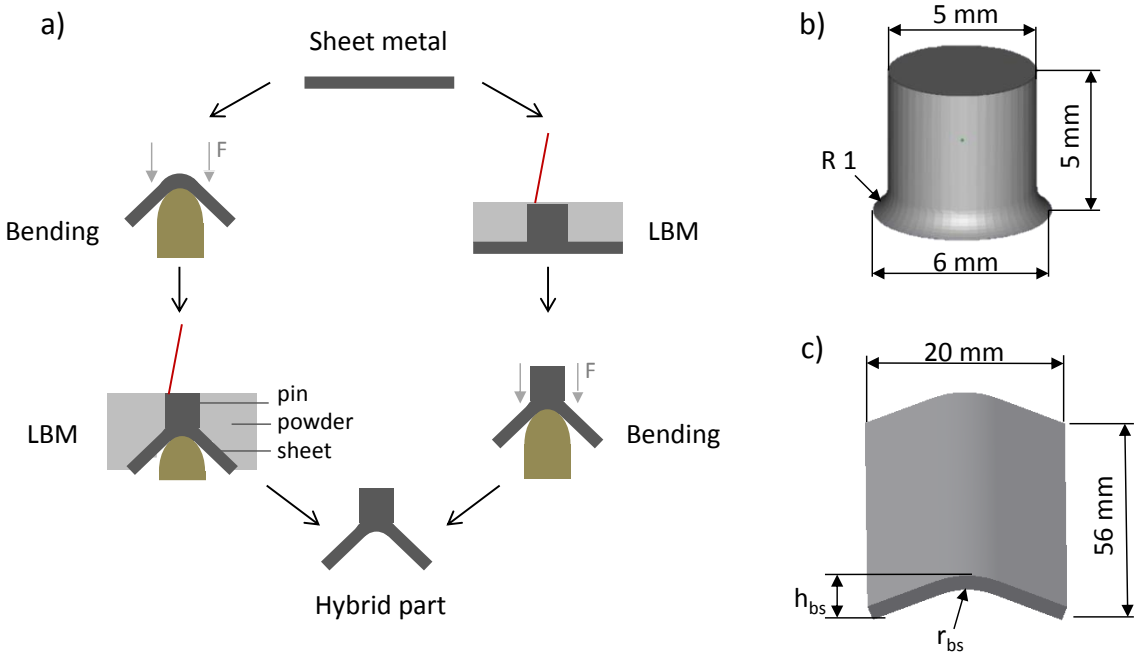

Fig. 1. a) Different process routes for the investigated process chain combining sheet metal bending and laser beam melting; b) dimensions of the LBM sample part; c) dimensions of the bending specimen with varied parameters

2.2. Bending

Regarding the left route in Fig. 1 a), rectangular specimens with a length of 56 mm and a width of 20 mm (see Fig. 1 c) were cut out from bigger sheets by laser cutting. These specimens were used for warm bending at a temperature of 250 °C. The bending tool is described in more detail elsewhere (Merklein et al., 2016). The resulting bending specimens used for the following LBM process are characterized by different combinations of sheet thickness t_0, bending radius r_{bs} and height h_{bs} (distance from top to bottom edge), which depends on the displacement of the die. Table 1 gives an overview of the investigated samples. For the right sequence in Fig. 1 a), bending was performed at a temperature of 400 °C, because preliminary tests yielded higher formability of hybrid samples at this temperature.

Table 1. Parameters of the investigated bending specimens

Specimen	Sheet thickness t_0 (mm)	Bending radius r_{bs} (mm)	Height h_{bs} (mm)
A	1.0	7	4.1
B	1.5	7	4.7
C	1.0	3	2.8
D	1.5	3	3.0

2.3. LBM process

For the LBM process, inert gas atomized Ti-6Al-4V powder from AP&C Advanced Powders and Coatings Inc. with spherical shape and a mass-median-diameter of 30 µm was used. The chemical composition of the powder was checked by energy-dispersive X-ray spectroscopy. Before usage, the powder was dried to avoid moisture. The LBM machine SLM 280HL from SLM Solutions GmbH was used, equipped with an Ytterbium fiber laser with a maximum power of 400 W and a beam diameter of approximately 80 µm in focus. All experiments were performed using a layer thickness of l_z = 50 µm, a hatch distance of h_s = 120 µm and using Argon as process gas. Three laser parameter sets differing in laser power P_L and scan speed v_s were used (see Table 2). The macroscopic energy density E_V for these parameter sets is calculated according to

$$E_V = \frac{P_L}{v_s \cdot l_z \cdot h_s}, \qquad (1)$$

and listed as hint for the accumulated heat. A silicon lip was used for recoating the powder layers. The geometry which has to be built in the LBM process is shown in Fig. 1 b). It has a cylindrical shape with a height of 5 mm. The diameter at the top is 5 mm and broadens to 6 mm by a fillet radius at the bottom, which leads to a smooth transition to the sheet to avoid cracks occurring at the transition zone (Ahuja et al., 2015).

Table 2. Investigated laser parameter sets for LBM

Parameter set	Power P_L (W)	Scan speed v_s (mm/s)	Energy density E_V (J/mm³)
I	250	900	50
II	250	300	140
III	400	300	220

2.3.1. LBM on flat sheets

To perform LBM on flat sheets, bigger square-shaped sheets with a side length of 277 mm were used in order to manufacture 20 homogeneously distributed samples at the same time. These sheets are clamped with screws at the margin on a stainless steel substrate plate with a thickness of 25 mm which is again mounted on a 200 °C-heated base plate (Schaub et al., 2016). However, temperature measurements with thermocouples showed that only 170 °C is reached at the titanium sheet. After LBM, the samples were brought into the final shape for bending (56 x 20 mm²) by laser cutting around the pins.

2.3.2. LBM on bent sheets

Processing multiple bending specimens with the different dimensions listed in Table 1 at the same time is challenging because the top edges of the samples have to be brought to the same height level in order to assure proper recoating. Fig. 2 shows the developed clamping device which was used for the experiments. Twelve slots were milled in a standard substrate plate, which can be loaded with punches that are adjusted to the radius and sheet thickness of the respective bending specimen. Fixation metal sheets are screwed to clamp the samples from above. The heights of the top edges of the sample are adjusted using metal foils of

different thicknesses as spacers beneath the punches and are checked with a tactile distance meter. In this way the heights of the samples can be levelled with accuracy in the order of one layer thickness (50 µm).

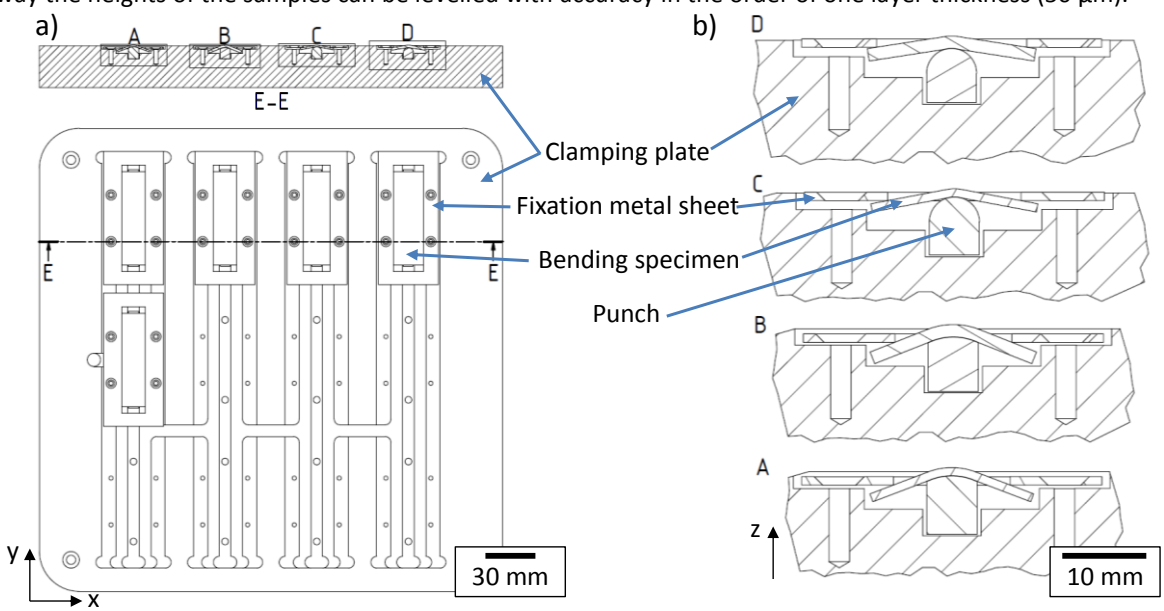

Fig. 2. a) Modular clamping device; b) detailed views of exemplarily mounted bending specimens according to Table 1

2.4. Mechanical characterization

Shear testing was chosen for characterizing the connection strength between additive part and sheet. The testing setup is schematically presented in Fig. 6 a). The hybrid part is fixed between two baseplates and the additive element is sheared off along the long edge of the sheet by a moving die. The displacement and force of the die are logged and the maximum force of failure taken to compare the samples. Bending specimens with a sheet thickness of t_0 = 1.5 mm and a bending radius of r_{bs} = 3 mm were used for the tests. In former work, heat treatment of hybrid parts according to (Vrancken et al., 2012) yielded higher connection strength than for untreated samples. For this reason, all tested samples in this work were heated up to 850 °C within 1.5 h and held for 2 h at this temperature. Afterwards, the samples were allowed to cool down in the furnace. The whole procedure was conducted using Argon to avoid strong oxidation.

3. Results and Discussion

3.1. Phenomenological comparison between the process routes

Looking at the two different process routes sketched in Fig. 1 a), the resulting hybrid parts will presumably differ depending on which sequence is chosen. In each case, the first step of the sequence complicates the second one. When bending is performed after LBM, the formability of the sheet is reduced by the additive element. Preliminary bending tests showed that bending angles, which lead to samples listed in Table 1, are not achievable. While for bending before LBM, a displacement of the die of 4.5 mm (bending specimen A and B) or 2 mm (C and D) was used, a value of only 1.5 mm could be applied after LBM.

When LBM is performed after bending, the uneven top surface makes it challenging to build the pin on top of a bending specimen. Taking bending specimen A, the height variation within the irradiated area is approximately 0.5 mm, which is tenfold the used layer thickness. This problem can be circumvented to a certain extent, because the elastic recoating lip allows leveling the powder layer beneath the highest point of the sample (see Fig. 3). The first layer was therefore manually adjusted in a way that only around 70 percent of the diameter of the irradiation zone was covered with powder. This reduces the height of the powder layer at the margin. On the other hand this leads to re-melting the center area several times without powder on top.

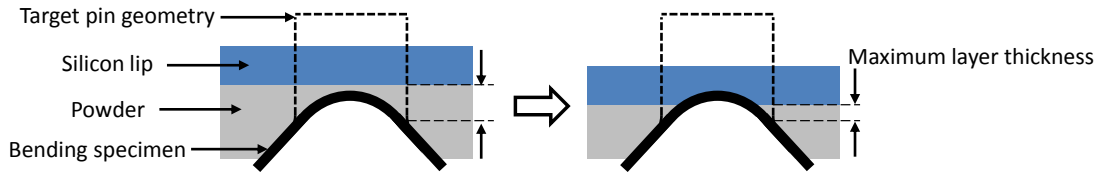

Fig. 3. Sketch of the layer adjusting procedure using an elastic silicon lip to reduce the thickness of the powder layer at the peripheral zone (moving direction of the silicon lip perpendicular to the image plane). The pin dimensions are exaggerated for better visualization.

Fig. 4 shows produced hybrid samples when LBM is performed after bending. All shown samples, which cover the different bending parameters of Table 1, were simultaneously produced. This proves the feasibility of the modular clamping device to be able to build on different shaped samples in the same LBM process.

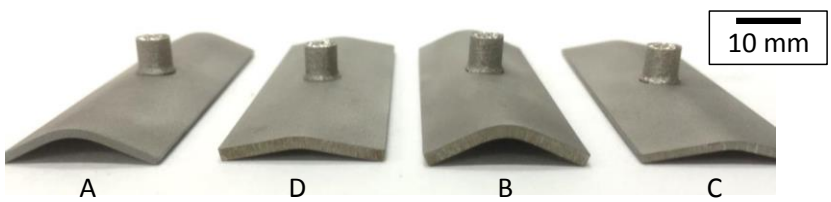

Fig. 4. Hybrid samples fabricated in the same build job of LBM after bending. Nomenclature according to Table 1

The bending parameter set B is chosen for metallographic analysis, as its samples show a strong height variation in the irradiated area. In Fig. 5, etched samples of this parameter set (c, d) are compared with hybrid samples of the other process route right after the LBM process (a, b). Furthermore two different laser parameter sets are compared. Parameter set (I) with P_L = 250 W, vs = 900 mm/s is a standard set to obtain parts with a good relative density above 99.5 %, while parameter set (III) with P_L = 400 W, vs = 300 mm/s exhibits an excessive energy density which leads to a higher porosity (Schaub et al., 2016). Note that in Fig. 5 pores cannot be properly identified. From images c) and d) it can be extracted that the described layer adjusting procedure makes it possible to balance a height variation of 0.2 mm for laser parameter set (I) and 0.4 mm for parameter set (III). The difference is based on the fact that with higher laser power and lower scan speed (that is higher energy density) the melt pool is penetrating deeper the powder layer and substrate. From subfigure c) and d) it can be seen that powder was not properly molten at the outer margin, which results in a non-smooth transition.

The influence of the laser parameter set on the microstructure in the additive part can also be seen in Fig. 5. With high laser power and low scan speed very pronounced columnar β grains in vertical direction arise, while at lower laser power and higher scan speed a fine structure is visible. The coarser prior grain structure with higher energy input is in accordance to literature (Thijs et al., 2010), where it is attributed to the influence of the melt pool size. In Fig. 5 b) and d), a significantly increased melt pool depth can be seen in

comparison to a) and c). Furthermore a distinct heat affected zone with irregular boundary shape appears (white area). A closer look at the microstructure is presented in Fig. 7, and will be discussed in the following chapter.

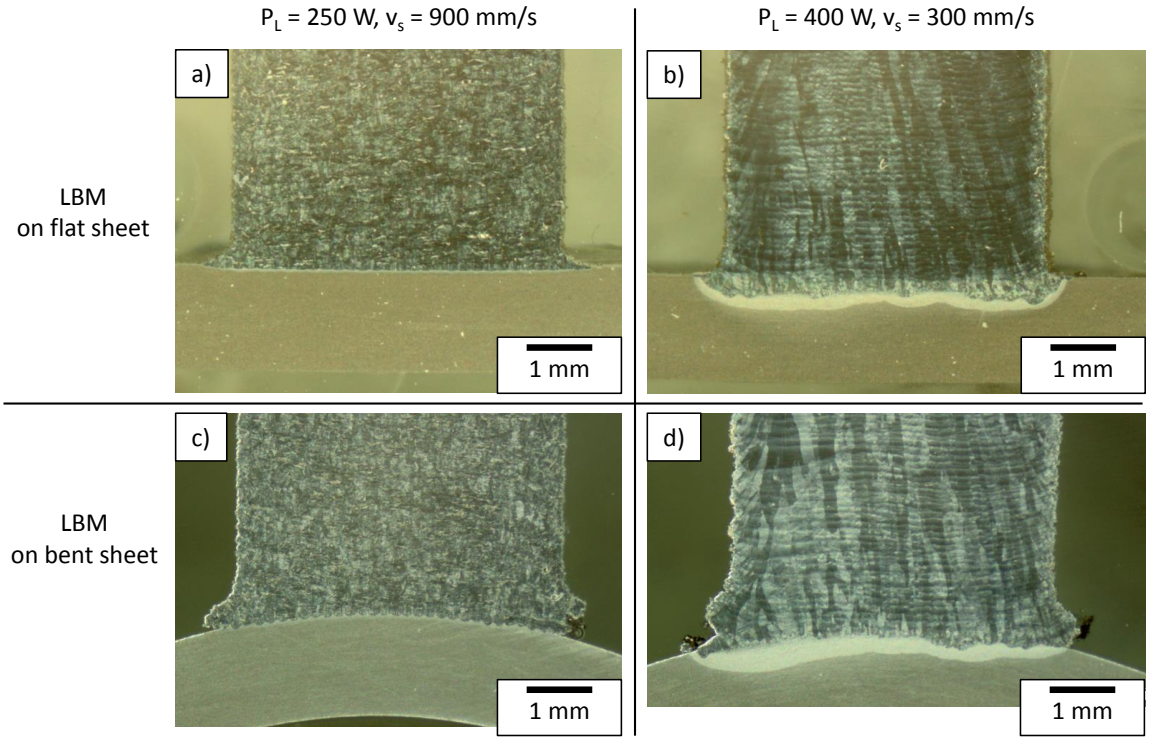

Fig. 5. Etched hybrid samples after LBM with a constant sheet thickness of t_0 = 1.5 mm

3.2. Mechanical characterization

In order to characterize the mechanical properties of hybrid parts, shear tests were carried out. In Fig. 6 b), the maximum shear force is plotted for the different process routes and laser parameters. For comparison, values of completely laser beam melted parts and machined parts from former experiments of (Schaub et al., 2016) are included. These parts were manufactured using the same pin geometry but with a flat base. The completely additive part was built using a laser beam power of 250 W and a scan speed of 900 mm/s, which is identical to the used parameter set (I) for the hybrid specimens.

As a major finding, it can be seen from Fig. 6 that the process route has no distinct influence on the shear strength of the hybrid parts due to high deviation. This is a surprising fact as like explained earlier the processing conditions of the different routes differ to a large extent. Even though the range of single measurements, indicated by the error bars, is rather high, a slight tendency of higher maximum shear force with higher laser energy density can be observed.

For a proper comparison, the force-resisting area had to be taken into account to calculate the shear strength. However, the force-resisting area cannot be determined accurately regarding porosity or the improper connection at the margin zone when conducting LBM after bending (c.f. lower images in Fig. 5), which too is dependent on the laser parameters. Nevertheless, the pin diameter above the connection zone

can be determined. While for parameter set (I) the real pin diameter matches the nominal diameter of 5 mm with an accuracy of 20 µm, for set (III) the real value exceeds the nominal value by 3.5 %.

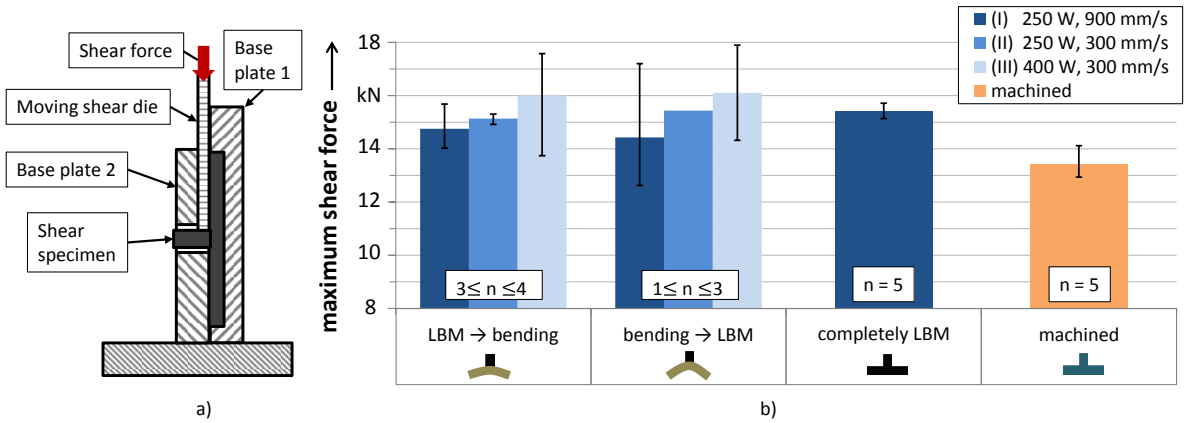

Fig. 6. a) Shear testing setup; b) results of the mechanical characterization of hybrid samples. The thickness of the sheet or respectively base is t_0 = 1.5 mm, the bending radius is r_{bs} = 3 mm. Error bars indicate the range of single measurements. Reference values of machined and purely LBM parts according to (Schaub et al., 2016)

The reason for this is that a higher energy density leads to a broader melt pool and enlarges the real size of the pin diameter, because the same track width compensation was used for all experiments. If one just accounts the real diameter above the connection zone, shear strength can be calculated. For parameter set (III) this leads to a value of 760 MPa (LBM-bending) and 765 MPa (bending-LBM), while parameter set (I) exhibits shear strengths of 750 MPa and 730 MPa, respectively. As the results of single measurements scatter in a range of up to 200 MPa, no significant trend between the laser parameter sets can be observed. Still, minor differences could originate from the laser penetration depth which varies to a large extent (see Fig. 5). In former work on flat sheets, it was shown that an excessive input energy leads to high porosity (Schaub et al., 2016), which usually implies a lower maximum load. The positive effect of deep penetration depth might balance the negative effect of porosity in the connection zone.

To further elucidate possible differences between the laser parameter sets, a closer look at the microstructure of hybrid samples after LBM on flat sheets was taken (see Fig. 7). In literature, it can be found that, besides prior columnar β grains, rapid cooling in LBM usually leads to a fine acicular α' martensite (Thijs et al., 2010), which can rudimentarily be seen in subfigure a) and b). However, (Xu et al., 2015) demonstrated that in situ martensite decomposition can take place when LBM parameters are adjusted. While for laser parameter set (I) the columnar prior β grains can be seen, for set (III) the whole image lies inside one grain. After heat treatment, the microstructure shows a mixture of α (bright) and β (dark). Inside the additive part, globularization of α grains has already started. This is surprising, as globularization was expected to occur only for a higher temperature and residence time (Vrancken et al., 2012). No significant differences can be seen between the laser parameter sets in subfigure c) and d). This indicates that the heat treatment has a homogenizing effect and explains the minor differences in the mechanical results between different laser parameter sets. At the border of the heat affected zone, a transition from equiaxed α grains of the sheet material to the typical structure of the additive part such as in c) and d) can be seen. The α grains appear to somewhat larger near this transition zone for laser parameter set (III), but these small differences disappear after around 100 µm above the transition line. This again supports the assumption that the heat treatment aligns the microstructure of hybrid parts processed with widely varying LBM parameters. This was not expected, as the applied temperature (850 °C) lies beneath the β transus temperature. As grain

growth beneath the β transus is limited for LBM parts (Vrancken et al., 2012), differences between the laser parameter sets were expected.

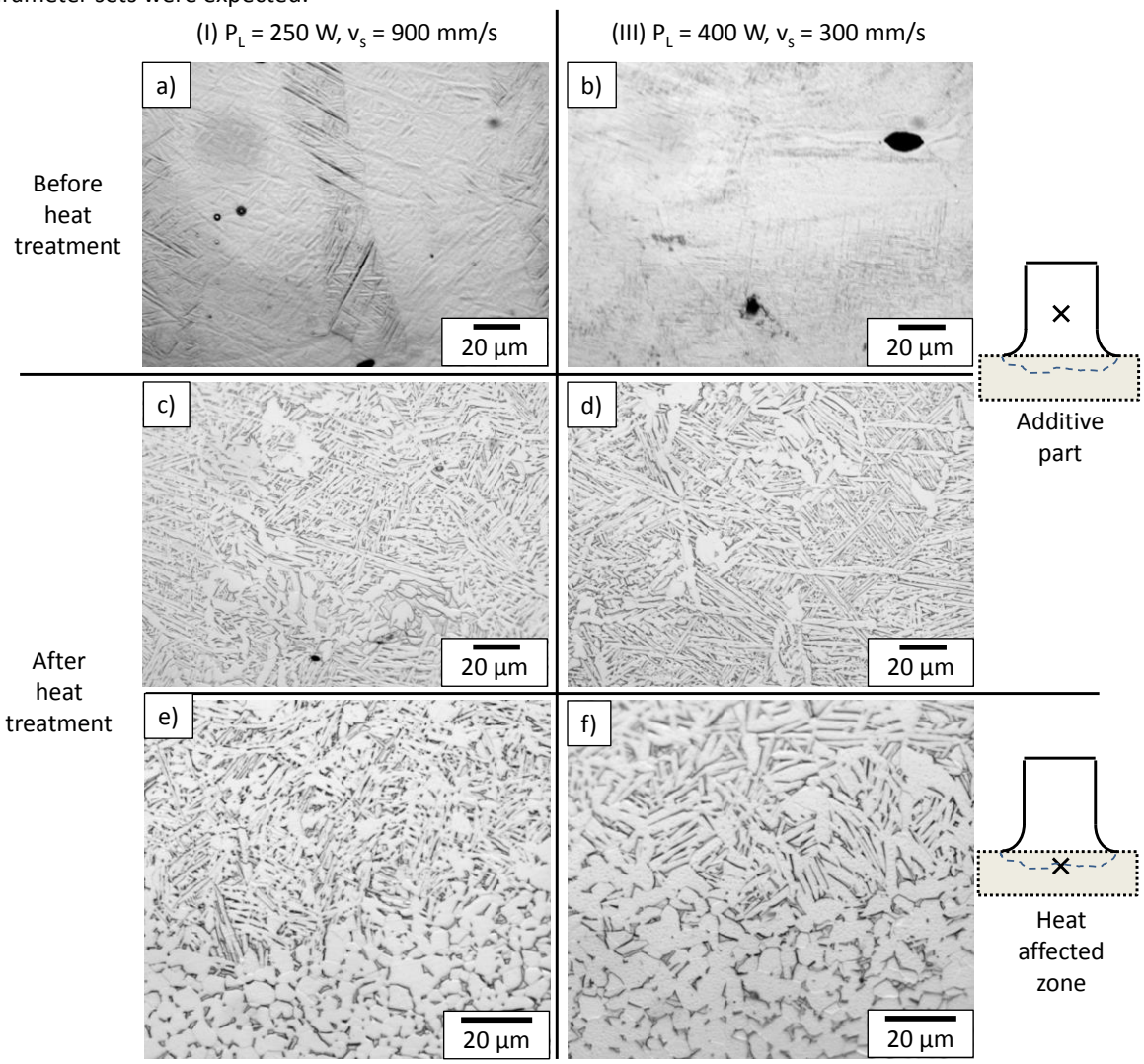

Fig. 7. Microstructure of hybrid parts (LBM on flat sheet) before (a,b) and after heat treatment (c-f) for laser parameter set (I) and (III). Images of (a-d) are taken from the center of the additive part, (e-f) from the transition zone between sheet and heat affected zone

4. Summary

A consecutive process chain was presented using laser beam melting and sheet metal bending of Ti-6Al-4V. Hybrid test samples were produced following both possible processing sequences. It was demonstrated that it is possible to use bent sheets with different thicknesses and bending radii as substrate in the same LBM process by using a modular clamping device. The problem of a big height variation of the substrate in the melting region can be circumvented by a certain extent by the elasticity of the used

recoating mechanism, but a weaker connection in the margin region remains. Different laser parameter sets showing a great variation in energy density were compared. With excessive energy input deep laser penetration and a large heat affected zone can be obtained for both process routes. Applying bending after the LBM process leads to a reduced formability of the sheets.

To quantify the connection strength between additive part and sheet, shear tests were performed. It was shown that the discussed problems and differences of the two process route surprisingly do not lead to significantly different connection strength of the hybrid parts. The tendency of a higher maximum shear force for increased laser energy input is mainly caused by the increased connection area resulting from a broader melt pool. Heat treatment, though beneath the β transus temperature, was shown to have a homogenizing effect, explaining the minor differences in shear strength between different energy densities in the LBM process. Still, a positive effect of deep laser penetration is assumed to balance negative effects of high porosity.

All in all, the connection strength is comparable to completely laser beam melted samples and even higher than machined specimens. This demonstrates that the presented hybrid manufacturing approach is suitable to produce parts with competitive connection strength.

Future work should focus on the impact of process conditions and different heat treatments on the microstructure and mechanical behaviour of the hybrid parts.

Acknowledgements

The authors would like to acknowledge the support provided for project B5 by DFG, the German Research Foundation under the collaborative research center, CRC 814 – Additive Manufacturing. Further, the authors gratefully acknowledge funding of the Erlangen Graduate School in Advanced Optical Technologies (SAOT) by the German Research Foundation (DFG) in the framework of the German excellence initiative.

References

Ahuja, B., Schaub, A., Karg, M., Schmidt, R., Merklein, M., Schmidt, M., 2015. High power laser beam melting of Ti6Al4V on formed sheet metal to achieve hybrid structures, in: Proc. of SPIE Vol. 9353. Presented at the Laser 3D Manufacturing II, San Francisco, California, United States, p. 93530X. doi:10.1117/12.2082919

Matena, J., Petersen, S., Gieseke, M., Kampmann, A., Teske, M., Beyerbach, M., Escobar, H.M., Haferkamp, H., Gellrich, N.-C., Nolte, I., 2015. SLM Produced Porous Titanium Implant Improvements for Enhanced Vascularization and Osteoblast Seeding. International Journal of Molecular Sciences 16, 7478–7492. doi:10.3390/ijms16047478

Merklein, M., Dubjella, P., Schaub, A., Butzhammer, L., Schmidt, M., 2016. Interaction of Additive Manufacturing and Forming, in: Drstvenšek, I., Drummer, D., Schmidt, M. (Eds.), Proceedings of 6th International Conference on Additive Technologies. Presented at the 6th International Conference on Additive Technologies iCAT 2016, Nürnberg, Germany, pp. 309–316.

Schaub, A., Ahuja, B., Butzhammer, L., Osterziel, J., Schmidt, M., Merklein, M., 2016. Additive Manufacturing of Functional Elements on Sheet Metal. Physics Procedia, Laser Assisted Net Shape Engineering 9 International Conference on Photonic Technologies Proceedings of the LANE 2016 September 19-22, 2016 Fürth, Germany 83, 797–807. doi:10.1016/j.phpro.2016.08.082

Schrage, J., 2016. Maschinenspezifische Kostentreiber bei der additiven Fertigung mittels Laserstrahlschmelzen (LBM), in: Kniffka, W., Eichmann, M., Witt, G. (Eds.), Proceedings of the 13 Th Rapid.Tech Conference. Presented at the Rapid.Tech – International Trade Show & Conference for Additive Manufacturing, Erfurt, Germany, p. 72.

Thijs, L., Verhaeghe, F., Craeghs, T., Humbeeck, J.V., Kruth, J.-P., 2010. A study of the microstructural evolution during selective laser melting of Ti–6Al–4V. Acta Materialia 58, 3303–3312. doi:10.1016/j.actamat.2010.02.004

Vrancken, B., Thijs, L., Kruth, J.-P., Van Humbeeck, J., 2012. Heat treatment of Ti6Al4V produced by Selective Laser Melting: Microstructure and mechanical properties. Journal of Alloys and Compounds 541, 177–185. doi:10.1016/j.jallcom.2012.07.022

Xu, W., Brandt, M., Sun, S., Elambasseril, J., Liu, Q., Latham, K., Xia, K., Qian, M., 2015. Additive manufacturing of strong and ductile Ti–6Al–4V by selective laser melting via in situ martensite decomposition. Acta Materialia 85, 74–84. doi:10.1016/j.actamat.2014.11.028